Sustinere
Journal of Environment and Sustainability
Volume 8 Number 1 (2024) 44-53

Print ISSN: 2549-1245 Online ISSN: 2549-1253
Website: https://sustinerejes.com E-mail: sustinere.jes@uinsaid.ac.id

RESEARCH PAPER

Adsorption of iron and manganese from acid mine drainage by zalacca (*Salacca zalacca*) peel-activated carbon

Eka Masrifatus Anifah*, Ismi Khairunnissa Ariani, Janet Tio Panny Tindaon, Basransyah
Department of Environmental Engineering, Institut Teknologi Kalimantan, Indonesia

Article history:
Received 12 November 2023 | Accepted 1 April 2024 | Available online 20 May 2024

Abstract. The low pH and high metal concentration in acid mine drainage cause environmental problems and affect human health. Adsorption not only removes the pollutants but also increases pH levels. Natural adsorbents have gained attention because of their widespread availability, low cost, and effectiveness. Zalacca peel waste is among the biomass materials showing promise as activated carbon for removing contaminants from acid mine drainage. This study aims to investigate the adsorption capacity of activated carbon from zalacca peel for removing iron and manganese from acid mine drainage. Adsorption studies were conducted in batch experiments using various dosages and contact times. Optimal results were achieved with a dosage of 0.8 grams per 100 mL and contact time of 60 minutes, resulting in 80% removal efficiency for iron and 24% for manganese. The neutralization process occurred post-adsorption, bringing the final pH close to neutral levels, suitable for environmentally safe discharge. Experiment data were fitted to the Freundlich isotherm and pseudo-second order kinetics. FTIR analysis revealed functional groups including C-H, C-O, and C=C was found in the adsorbent. Furthermore, surface area and pore volume experienced slight increases following activation with KOH.

Keywords: Acid-mined drainage; activated carbon; adsorption; isotherm; kinetics; Zalacca peel

1. Introduction

The coal mining process generates wastewater containing high concentrations of heavy metals (Fe, Al, Mn, Cu, Zn, Pb), elevated sulfate concentration, and low pH. Acid mine drainage typically exhibits Fe (II) concentrations ranging from 9.4 mg/L – 20.5 mg/L, Mn (II) concentrations ranging from 8.1 mg/L – 23.12 mg/L, and a pH of range approximately 2 to 4 (Anshariah, 2016; Indra et al., 2014). High levels of Fe can lead to deposition of ferric oxide, which, upon reacting with oxygen in the water, can be lethal to aquatic life. Moreover, acid mine drainage contaminates surface water, groundwater, and soil, posing significant health risks to humans, decimating aquatic populations, and harming biodiversity (Kefeni et al., 2017).

Several approaches can be employed to treat acid mine drainage, including neutralization, coagulation-flocculation (Arifin et al., 2023), biological treatments (Rambabu et al., 2020) and adsorption (Yulianis et al., 2022). Among these methods, the adsorption is often preferred due to

*Corresponding author. E-mail: ekamasrifatus@itk.ac.id
DOI: https://doi.org/10.22515/sustinere.jes.v8i1.366

its cost-effectiveness (Masukume et al., 2014) and its efficiently removal of pollutants from wastewater (Burakov et al., 2018). Adsorption is a physicochemical process that utilizes adsorbents to remove contaminants from acid mine drainage.

The adsorption process offers several advantages, particularly its ability to operate effectively across a wide pH range, making it suitable for treating acid mine drainage characterized by low pH levels (Sadegh & Ali, 2018). Adsorbent capable of adsorbing dissolved substances from wastewater. Various factors influence the efficiency of adsorption, including pH, contact time, initial ion concentration, and adsorbent dosage (Iftekhar et al., 2018). Activated carbon is among the most commonly used adsorbents. Additionally, natural adsorbents are increasingly utilized in acid mine drainage treatment due to their abundance and high removal efficiency. For instance, sugarcane bagasse achieved a 79.65% removal of Fe (Imani et al., 2021) and a 60% removal of Mn, while meranti sawdust demonstrated remarkable removal rates of 99.9% for Fe and 92.9% for Mn (Busyairi et al., 2019). Orange peel also exhibits notable efficiency, achieving an 82.99% removal of Fe (Fatmawati et al., 2019). Salacca Zalacca peel shows potential as an adsorbent due to its cellulose, hemicellulose, and lignin content. Previous studies have demonstrated its ability to Pb by 96.82% (Hanifah & Hadisoebroto, 2021) and Cr by 69.45% (Purnamaningsih et al., 2017).

Chemical activation is a process used to increase surface area and pore volumes by introducing acid or base solutions such as H_3PO_4, H_2SO_4, NaOH, NaCI, HCI, and $ZnCI_2$ (Bijang et al., 2019). KOH is commonly used activator that can significantly increase the surface area of adsorbents to up to 3000 m^2/g, with an adsorption capacity of up to 686.6605 mg/g (Utama et al., 2016). This study aims to analyze the adsorption capacity of Zalacca (*Salacca Zalacca*) peel carbon activated by KOH for removal of Fe and Mn from acid mine drainage.

2. Material and methods

2.1. Activated carbon preparation

Zalacca peels were collected from the waste of a home industry in Balikpapan. Initially, the peels were cut into small pieces and cleaned using distilled water (aquadest). Subsequently, they were dried in an oven at 105°C for 24 hours. In next step, the dried zalacca peels were carbonized in a furnace at 300°C for 30 minutes. The resulting zalacca peel carbon was then mixed with 3 M KOH (anhydrous, Smart Lab) at a ratio of 1:4 (w/v). This mixture was stirred for 4 hours on a hotplate at 80°C and left to soaked for an additional 24 hours. Following activation, the activated carbon was washed using distilled water until the rinse water reached a pH of 6-7. Finally, the activated carbon was dried at 105°C for 3 hours and sieved to achieve a particle size of 100 mesh.

2.2. Adsorption experiments

In this experiment, a batch system was utilized. $FeSO_4$ (Smart Lab) and $MnSO_4$ (Smart Lab) were employed to create synthetic acid-mined drainage. HCl (Smart Lab) was used to adjust the pH of acid-mined drainage to 3. The synthetic acid mined drainage had an iron concentration of 10 mg/L, a manganese concentration of 5 mg/L, and a pH of 4. To conduct the experiment, 100 mL of synthetic acid-mined drainage was mixed with adsorbent in orbital shaker at stirring rate of 100 rpm. The dosage of the adsorbent ranged from 0.2 – 1.0 gram/100 mL, and a contact time ranged from 15-75 minutes during the batch experiment. Following mixing, the filtrate was passed through Whatman filter paper 40 using a vacuum pump. The concentrations of Fe and Mn in filtrate after adsorption were measured using a spectrophotometer (Spectroquant Prove 300). The experiment was conducted in duplo.

The efficiency of Fe and Mn removal and adsorption capacity were determined by equations (1) and (2).

$$\text{Removal efficieny (\%)} = \frac{C_0 - C_1}{C_0} \times 10 \quad (1)$$

$$\text{Adsorption capacity } (q) = \frac{C_o - C_1}{M} \times V \quad (2)$$

The adsorption capacity (q), which is used in isotherm determination, is calculated based on the mass of adsorbent (M) and the volume of solution (V). C_o and C_1 represent the initial concentrations prior to and after the adsorption process, respectively, measured in mg/L. q represents the total of adsorbed adsorbate on the absorbent, measured in (mg/g). The data obtained from batch experiments were analyzed using isotherms and kinetics. Freundlich and Langmuir isotherms were modeled using non-linear and linearization isotherm equations (3, 4) and (5, 6), respectively.

$$q_e = K_f \, C_e^{\frac{1}{n}} \quad (3)$$

$$Log\ q_e = Log\ K_f + \frac{1}{n}\ Log\ C_e \quad (4)$$

$$q_e = \frac{q_m\ K_L\ C_e}{(1 + K_L\ C_e)} \quad (5)$$

$$\frac{C_e}{q_e} = \frac{C_e}{q_m} + \frac{1}{K_L\ q_m} \quad (6)$$

C_e (mg/L) represents the concentration of adsorbate in equilibrium, and q_e (mg/g) corresponds to the capacity of adsorption. The coefficient of the Freundlich isotherm is represented by K_f and $1/n$, which are determined from the intercept and slope of the Freundlich isotherm plot with Log C_e on the x-axis and Log q_e ordination the y-axis. q_m corresponds to the maximum adsorption capacity (mg/g). Similarly, for the Langmuir isotherm, the parameter of q_m and K_L was determined from the intercept and slope by plotting C_e/q_m as an axis and C_e/q_e as an ordinate.

Pseudo-first order (7, 8) and pseudo-second order (9, 10) equations were utilized to determine the adsorption kinetics.

$$\frac{dq_t}{dt} = k_1\ (q_e - q_t) \quad (7)$$

$$Log\ (q_e - q_t) = Log\ q_e - \frac{k_1}{2.303}\ t \quad (8)$$

$$\frac{dq_t}{dt} = k_2\ (q_e - q_t)^2 \quad (9)$$

$$\frac{t}{q_t} = \frac{1}{k_2 q_e^2} + \frac{1}{q_e}\ t \quad (10)$$

q_e (mg/g) represents the adsorption capacity equilibrium, and q_t (mg/g) corresponds to the adsorption capacity at time t (in minutes). k_1 and k_2 represent the kinetic rate constants for pseudo-first order and second-first order, respectively.

2.3 Adsorbent characterization

FTIR (Bruker, ALPHA II) analysis was applied to investigate the functional group of adsorbents before and after activation using KOH. The FTIR analysis utilized a wavelength range of 1000-3500 cm^{-1}. The FTIR spectra were plotted as a function of transmittance and wavenumber. The surface area of adsorbents before and after activation was analyzed using the Brunauer–Emmett–Teller instrument (Quantachrome TouchWin).

3. Result and discussion

3.1. Effect of adsorbent dosage on Fe and Mn removal efficiency

Figure 1 illustrates the influence of adsorbent dosage on the efficiency of iron (Fe) and manganese (Mn) removal. It is evident that increasing the dosage from 0.2 to 0.8 g/100 mL gradually raised the removal efficiency from 88.20% to 97.19% for Fe and from 81.67% to 92.31% for Mn. The increase in dosage enhances the surface area, thereby providing more active sites for adsorption (Zhang et al., 2014). However, a further increase in dosage to 1.0 g/100 mL resulted in a slight decrease in removal efficiency of Fe and Mn by 0.89% and 1.2%, respectively. The decline can be attributed to agglomeration of adsorbent particles at higher dosages, which negatively affects the removal efficiency (Mosoarca et al., 2020; Yushin et al., 2019).

The preferential absorption of Fe over Mn can be explained by the higher concentration of Fe compared to Mn in aqueous solution. Higher concentrations generally lead to increased adsorption rates due to a greater abundance of adsorbate in the solution. Additionally, the ionic radius of the metals plays a role in adsorption performance, with iron a significantly lower ionic radius than manganese. The smaller ionic radius allows Fe to more easily penetrate the pores of the adsorbent (Bin Jusoh et al., 2005; Indah et al., 2016; Suliestyah et al., 2021).

Statistical analysis using one-way ANOVA with a 95% interval yielded a *p*-value of 0.000, indicating that the dosage has a significant effect on the efficiency of Fe and Mn removal.

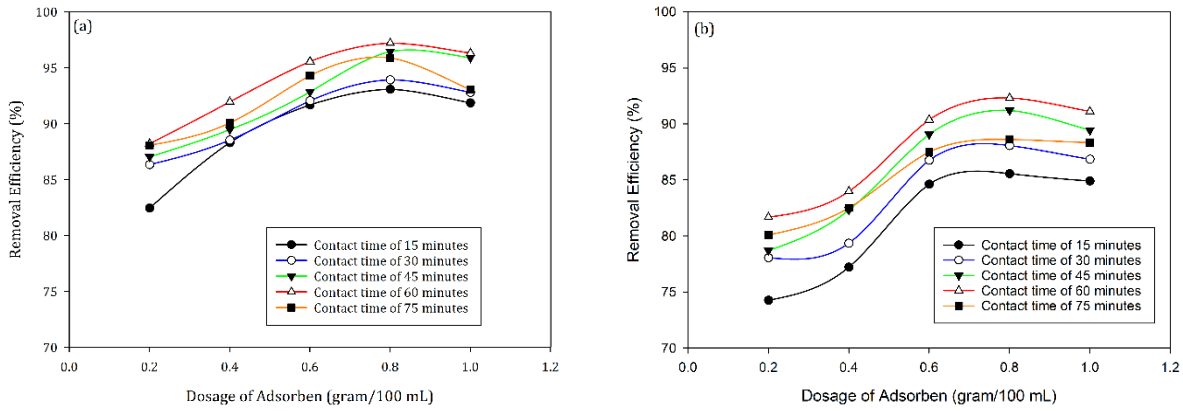

Figure 1. The effect of adsorbent dosage ranging from 0.2 – 1.0 g/100 mL on the removal efficiency of Fe (a) and Mn (b)was studied under initial Fe concentration of 10 mg/L and initial Mn concentration of 5 mg/L.

The pH of a solution significantly influences the interaction and surface charge between adsorbate and adsorbent. Figure 2 illustrates how the dosage of adsorbent affects the final pH after adsorption. The addition of zalacca activated carbon resulted in an increase in the final pH post-adsorption. Specifically, the initial pH of 3 rose to a range of 6.73 – 7.57 upon mixing. As the adsorbent dosage increased, so did the pH of the solutions. This finding corroborates a previous study that utilized natural clay to eliminate heavy metals from acid mine drainage (Esmaeili et al., 2019). The increasing final pH suggests a neutralization process occurred. This was likely due to the release of OH ions and gradual dissolution of the sorbent, consequently increasing the solution's pH (Hamayun et al., 2014; Iakovleva et al., 2015).

3.2. Effect of contact time on Fe and Mn removal efficiency

The determination of an optimal adsorption contact time for maximizing the efficiency of the adsorption process. Figure 3 illustrates the impact of adsorption contact time on the removal efficiency of iron and manganese. At the optimal dosage of 0.8 g/100 mL, the removal efficiency of Fe increased gradually from 93.07% to 97.19% at a contact time ranging from 15 to 60 minutes.

Simultaneously, the removal efficiency of Mn exhibited a sharp increase from 85.56% to 92.31% within the first 60 minutes. This observation demonstrates that extending the contact time enhances the adsorption capacity, with the highest removal efficiency achieved at 60 minutes.

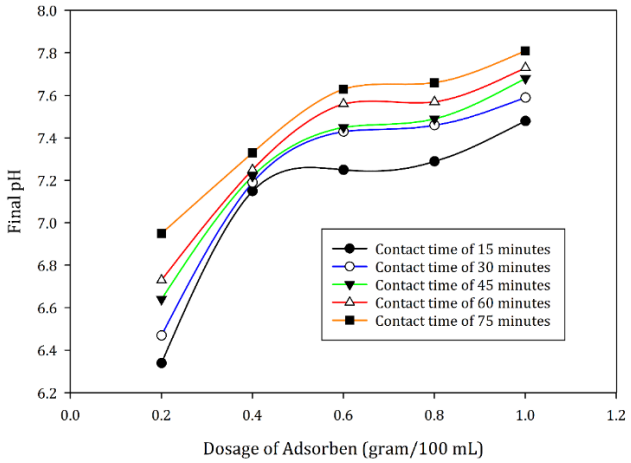

Figure 2. The effect of adsorbent dosage (0.2 – 1.0 g per 100 mL) on final pH with pH of 3 at the initial condition

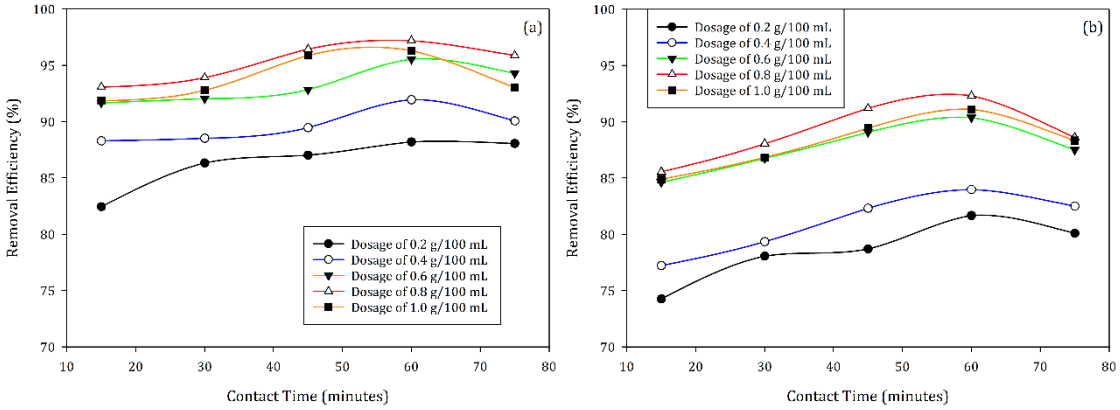

Figure 3. The effect of contact time of 0.2 – 1.0 g/100 mL on Fe (a) and Mn (b) removal efficiency; initial Fe concentration of 10 mg/L; initial Mn concentration of 5 mg/L

The initial rapid adsorption rate can be attributed to the abundance of available active sites compared to the metal adsorbate in the solution (Kampalanonwat & Supaphol, 2014; Panda et al., 2017). However, further increasing the contact time to 75 minutes resulted in a decrease in Fe and Mn removal efficiency dropped by 1.31% and 3.7%, respectively. The decline in efficiency may be due to the saturation of adsorbent surface sites, causing a higher concentration of ions on the absorbent surface than in the solution, leading to the release of Fe and Mn back into the solution (Irawan & Rumhayati, 2014). Statistical analysis with a confidence interval of 95% and *p*-value of 0.423 (Fe) and 0.290 (Mn) suggests that contact time duration does not significantly influence the efficiency of Fe and Mn removal.

3.3 Adsorption isotherm

Adsorption isotherm elucidate the equilibrium relationship between solute and adsorbent. The adsorption isotherm for iron and manganese in binary systems were fitted using Freundlich and Langmuir models. Table 1 presents the adsorption isotherm of Fe and Mn using zalacca peel-

activated carbon in equilibrium. Notably, the correlation coefficient (R^2) value for the Freundlich model exceeded that of Langmuir model. Therefore, the adsorption of Fe and Mn onto zalacca-activated carbon aligns with the Freudnlich isotherm. Previous studies have similarly demonstrated that the adsorption of Fe and Mn using chitosan derived from shrimp shells and magnetite graphene oxide best fits the Freundlich isotherm (Ali et al., 2018; Yan et al., 2014). The Freundlich isotherm characterized the heterogeneity of active binding sites on the surface of adsorbents. This heterogeneous arises from varied oxygen-containing functional groups (such as carboxyl, hydroxyl) with distinct levels of activity and adsorption energy degrees (Zhan et al., 2018).

Table 1. Adsorption isotherm of Fe and Mn using activated carbon from zalacca peel

Isotherm		Fe (II)	Mn (II)
Freundlich	R^2	0.882	0.831
	K_f	3.278	1.784
	1/n	0.955	0.920
	n	1.047	1.086
Langmuir	R^2	0.0009	0.272
	q_m	204.082	2.556
	K_L	0.016	0.409

The coefficients of K_f and $1/n$ were derived from the Freundlich isotherm model. K_f represents the amount of adsorbate that is adsorbed per unit mass of adsorbent. Iron exhibited a slightly higher K_f value than Mn, suggesting that zalacca activated carbon absorbed more Fe than Mn. The obtained values of $1/n$ for both Fe and Mn are less than 1 ($1/n < 1$), indicating that the adsorption energy decreases with increasing surface concentration (Can et al., 2016; Chen et al., 2022). Furthermore, a $1/n$ value less than implies favorable absorption, as the contact angle is indicative of favorable absorption when $1/n < 1$ (Adekola et al., 2016). Therefore, the adsorption of both metals on zalacca activated carbon is considered favorable.

3.4 Adsorption kinetics

Adsorption kinetics elucidates the rate at which adsorbate molecules are transferred to the surface of the adsorbent surface. First-pseudo-order and second-pseudo-order kinetics were modeled using on experimental data at an optimal dosage of 0.8 grams per100 mL to determine the transfer mechanism occurring during adsorption. Table 2 displays the correlation coefficient (R^2), kinetics constants, and adsorption capacities (q_e) obtained from first-pseudo-order and second-pseudo-order kinetics models.

Table 2. Adsorption kinetics of Fe and Mn adsorption using zalacca peel activated carbon

Adsorption Kinetics		Fe (II)	Mn (II)
First-pseudo-order	R^2	0.054	0.041
	k_1 (min^{-1})	0.005	0.015
	$q_{e\,cal}$ (mg/g)	24.232	42.413
Second-pseudo-order	R^2	0.999	0.997
	k_2 (min^{-1})	1.461	6.574
	$q_{e\,cal}$ (mg/g)	1.303	0.613
	$q_{e\,exp}$ (mg/g)	1.300	0.620

The adsorption of Fe corresponded a stronger correlation with second-pseudo-order kinetics, supported by a higher correlation coefficient (R^2) of 0.999. In the binary metal system

with Fe, Mn adsorption also followed the second pseudo-order kinetics, displaying a correlation coefficient of 0.997. Previous studies similarly found that the Fe and Mn aligned most closely with the second pseudo-order kinetics (Zhang et al., 2014). Chemisorption was assumed to be involved in the pseudo-second-order kinetics (Kaveeshwar et al., 2018; Núñez-Gómez et al., 2020).

The pseudo-second-order order model suggests that adsorption capacity is directly proportional to the number of active sites on the surface of adsorbents (Hasan et al., 2021). The calculation of adsorption capacity using the pseudo-second- order model closely matches experimental results. A lower value of the rate constant k_2 signifies a higher adsorption rate (Anggriani et al., 2021; Erani et al., 2022). Consequently, in this study, the adsorption rate of Mn was found to be 4.5 times faster than of Fe.

3.5 Adsorbents characteristics

Figure 4 illustrates the FTIR spectrum of zalacca peel before and after activation with KOH. The spectrum indicates that the activated carbon exhibited functional groups including C=C (1574.87 cm^{-1}), C-O (1300-1000 cm^{-1}), and C-H (747.36 cm^{-1}). Previous studies have also identified similar functional groups in the zalacca peel (Fatimah et al., 2020; Hasanah et al., 2022). Following activation, several small peaks disappeared. KOH, as a chemical activator agent, removes impurities such as silica in activated carbon to improve its adsorbent characteristics (Le Van et al., 2019). The BET results in Table 3 support the argument that the activator enhanced the adsorbent properties. It is evident that the surface area, pore volume, and diameter of the activated carbon increased after activation with KOH, although not significantly.

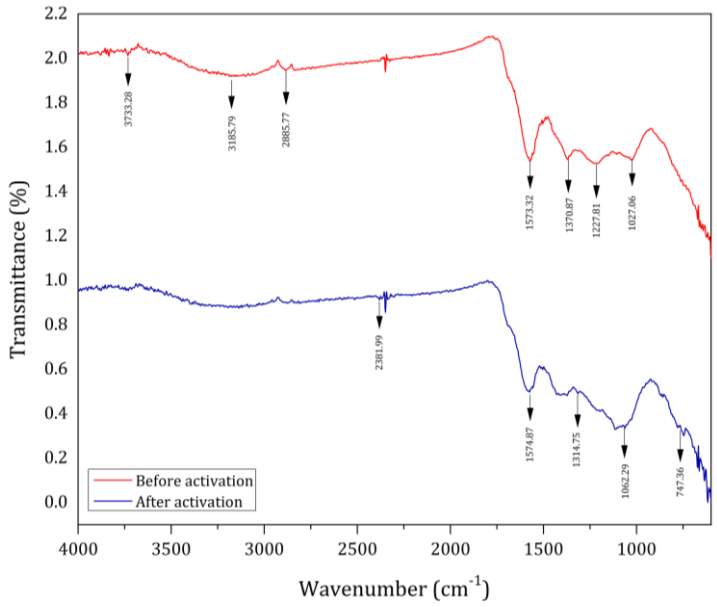

Figure 4. FTIR spectra of activated carbon (a) prior to activation and (b) afterward activation with KOH

Table 3. Data from Brunauer–Emmett–Teller (BET) analysis

Parameter	Unit	Before activation	After activation
Surface area	m^2/gram	0.116	0.173
Pore volume	cc/gram	0.0024	0.0038
Pore diameter	nm	49.62	54.17

4. Conclusion

The activation process removes impurities and modestly improves the pore volume and surface area of the adsorbent. The activated carbon derived from zalacca peel demonstrated effective removal of iron and manganese ions from the acid mine drainage. Additionally, a neutralization process occurs during adsorption, leading to an increase in the final pH of acid mine drainage post-treatment, rendering it safe for discharge into water bodies. According to the one-way ANOVA results, dosage significantly influences removal efficiency, whereas contact time shows no significant effect. Isotherms and kinetics studies suggest that the adsorption of iron and manganese on zalacca-activated carbon occurs on the heterogeneous of the adsorbent through chemisorption.

Acknowledgment

The authors are grateful to Direktorat Jenderal Pendidikan Tinggi, Riset, dan Teknologi, Kementerian Pendidikan, Kebudayaan, Riset, dan Teknologi Republik Indonesia for providing a research grant in 2023 with Penelitian Dosen Pemula (PDP) scheme.

References

Adekola, F. A., Hodonou, D. S. S., & Adegoke, H. I. (2016). Thermodynamic and kinetic studies of biosorption of iron and manganese from aqueous medium using rice husk ash. *Applied Water Science*, *6*(4). https://doi.org/10.1007/s13201-014-0227-1

Ali, M. E. A., Aboelfadl, M. M. S., Selim, A. M., Khalil, H. F., & Elkady, G. M. (2018). Chitosan nanoparticles extracted from shrimp shells, application for removal of Fe(II) and Mn(II) from aqueous phases. *Separation Science and Technology (Philadelphia)*, *53*(18). https://doi.org/10.1080/01496395.2018.1489845

Anggriani, U. M., Hasan, A., & Purnamasari, I. (2021). Kinetika Adsorpsi Karbon Aktif Dalam Penurunan Konsentrasi Logam Tembaga (Cu) dan Timbal (Pb). *Jurnal Kinetika*, *12*(2).

Anshariah, A. (2016). Studi Pengelolaan Air Asam Tambang Pada Pt. Rimau Energy Mining Kabupaten Barito Timur Provinsi Kalimantan Tengah. *Jurnal Geomine*, *1*(1), 46–54. https://doi.org/10.33536/jg.v1i1.9

Arifin, U. R. S., Jadid, M. M. E., & Widiono, B. (2023). Pengolahan Limbah Air Asam Tambang Emas Dengan Proses Netralisasi Koagulasi Flokulasi. *DISTILAT: Jurnal Teknologi Separasi*, *5*(2), 112–120. https://doi.org/10.33795/distilat.v5i2.42

Bijang, C. M., Nurdin, M., Tehubijulluw, H., Fransina, E. G., Uyara, T., & Suarti. (2019). Application of Ouw natural clay activated acid and base as adsorbent of Rhodamine B dye. *Journal of Physics: Conference Series*, *1242*(1). https://doi.org/10.1088/1742-6596/1242/1/012014

Bin Jusoh, A., Cheng, W. H., Low, W. M., Nora'aini, A., & Megat Mohd Noor, M. J. (2005). Study on the removal of iron and manganese in groundwater by granular activated carbon. *Desalination*, *182*(1–3), 347–353. https://doi.org/10.1016/j.desal.2005.03.022

Burakov, A. E., Galunin, E. V, Burakova, I. V, Kucherova, A. E., Agarwal, S., Tkachev, A. G., & Gupta, V. K. (2018). Adsorption of heavy metals on conventional and nanostructured materials for wastewater treatment purposes: A review. *Ecotoxicology and Environmental Safety*, *148*, 702–712. https://doi.org/10.1016/j.ecoenv.2017.11.034

Busyairi, M., Firlina, F., Sarwono, E., & Saryadi, S. (2019). Pemanfaatan Serbuk Kayu Meranti Menjadi Karbon Aktif Untuk Penurunan Kadar Besi (Fe), Mangan (Mn) Dan Kondisi Ph Pada Air Asam Tambang. *Jurnal Sains &Teknologi Lingkungan*, *11*(2), 87–101. https://doi.org/10.20885/jstl.vol11.iss2.art1

Can, N., Ömür, B. C., & Altındal, A. (2016). Modeling of heavy metal ion adsorption isotherms onto metallophthalocyanine film. *Sensors and Actuators, B: Chemical*, *237*. https://doi.org/10.1016/j.snb.2016.07.026

Chen, X., Hossain, M. F., Duan, C., Lu, J., Tsang, Y. F., Islam, M. S., & Zhou, Y. (2022). Isotherm models for adsorption of heavy metals from water - A review. In *Chemosphere* (Vol. 307). https://doi.org/10.1016/j.chemosphere.2022.135545

Erani, F. S., Hasan, A., & Purnamasari, I. (2022). Kinetika Adsorpsi Logam Cu dan Zn pada Limbah cair Kelapa Sawit Menggunakan Membran Silika. *KINETIKA*, *13*(03), 31–36.

Esmaeili, A., Mobini, M., & Eslami, H. (2019). Removal of heavy metals from acid mine drainage by native natural clay minerals, batch and continuous studies. *Applied Water Science*, *9*(4). https://doi.org/10.1007/s13201-019-0977-x

Fatimah, I., Sahroni, I., Dahlyani, M. S. E., Oktaviyani, A. M. N., & Nurillahi, R. (2020). Surfactant-modified Salacca zalacca skin as adsorbent for removal of methylene blue and Batik's wastewater. *Materials Today: Proceedings*, *44*. https://doi.org/10.1016/j.matpr.2020.11.440

Fatmawati, N., Usman, T., & Zahara, T. A. (2019). Bioadsorpsi Fe(II) oleh Kulit Buah Jeruk Citrus nobilis Lour. var microcarpa Termodifikasi Ca(OH)2. *Indonesian Journal of Pure and Applied Chemistry*, *1*(3). https://doi.org/10.26418/indonesian.v1i3.34205

Hamayun, M., Mahmood, T., Naeem, A., Muska, M., Din, S. U., & Waseem, M. (2014). Equilibrium and kinetics studies of arsenate adsorption by FePO4. *Chemosphere*, *99*. https://doi.org/10.1016/j.chemosphere.2013.10.075

Hanifah, H. N., & Hadisoebroto, G. (2021). Perbandingan Efektivitas Bioadsorben Berbagai Serbuk Kulit Buah Terhadap Logam Pb Dari Limbah Cair Laboratorium Farmasi. *Al-Kimia*, *9*(2), 188–200. https://doi.org/10.24252/al-kimia.v9i2.24660

Hasan, A., Yerizam, M., & Habib Yahya, M. (2021). Mekanisme Adsorben Zeolit dan Manganese Zeolit Terhadap Logam Besi (Fe). *Jurnal Kinetika*, *12*(01).

Hasanah, M., Wijaya, A., Arsyad, F. S., Mohadi, R., & Lesbani, A. (2022). Preparation of Hydrochar from Salacca zalacca Peels by Hydrothermal Carbonization: Study of Adsorption on Congo Red Dyes and Regeneration Ability. *Science and Technology Indonesia*, *7*(3). https://doi.org/10.26554/sti.202S2.7.3.372-378

Iakovleva, E., Mäkilä, E., Salonen, J., Sitarz, M., Wang, S., & Sillanpää, M. (2015). Acid mine drainage (AMD) treatment: Neutralization and toxic elements removal with unmodified and modified limestone. *Ecological Engineering*, *81*. https://doi.org/10.1016/j.ecoleng.2015.04.046

Iftekhar, S., Ramasamy, D. L., Srivastava, V., Asif, M. B., & Sillanpää, M. (2018). Understanding the factors affecting the adsorption of Lanthanum using different adsorbents: A critical review. *Chemosphere*, *204*(April), 413–430. https://doi.org/10.1016/j.chemosphere.2018.04.053

Imani, A., Sukwika, T., & Febrina, L. (2021). Karbon Aktif Ampas Tebu sebagai Adsorben Penurun Kadar Besi dan Mangan Limbah Air Asam Tambang. *Jurnal Teknologi*, *13*(1), 33–42. https://doi.org/10.24853/jurtek.13.1.33-42

Indah, S., Helard, D., & Yedriana, R. (2016). Pengaruh Variasi Konsentrasi Logam Mangan (Mn) terhadap Efisiensi Penyisihan Logam Besi (Fe) pada Adsorpsi Menggunakan Serbuk Kulit Jagung Sebagai Adsorben. *Jurnal Dampak*, *13*(2). https://doi.org/10.25077/dampak.13.2.100-106.2016

Indra, H., Lepong, Y., Gunawan, F., & Abfer-tiawan, M. S. (2014). Penerapan Metode Active dan Passive Treatmen dalam Pengelolaan Air Asam Tambang Site Lati. *Jurnal Sylva Lestari*, *1*(1), 1–9.

Irawan, C., & Rumhayati, B. (2014). Adsorption of Iron(II) By Fly Ash Adsorbent from Coal. In *J. Pure App. Chem.* Res (Vol. 3, Issue 3).

Kampalanonwat, P., & Supaphol, P. (2014). The study of competitive adsorption of heavy metal ions from aqueous solution by aminated polyacrylonitrile nanofiber mats. *Energy Procedia*, *56*(C). https://doi.org/10.1016/j.egypro.2014.07.142

Kaveeshwar, A. R., Ponnusamy, S. K., Revellame, E. D., Gang, D. D., Zappi, M. E., & Subramaniam, R. (2018). Pecan shell based activated carbon for removal of iron(II) from fracking wastewater: Adsorption kinetics, isotherm and thermodynamic studies. *Process Safety and Environmental Protection*, *114*. https://doi.org/10.1016/j.psep.2017.12.007

Kefeni, K. K., Msagati, T. A. M., & Mamba, B. B. (2017). Acid mine drainage: Prevention, treatment options, and resource recovery: A review. *Journal of Cleaner Production*, *151*, 475–493. https://doi.org/10.1016/j.jclepro.2017.03.082

Le Van, K., Thu, T. L. T., Thu, H. N. T., & Van Hoang, H. (2019). Activated Carbon by KOH and NaOH Activation: Preparation and Electrochemical Performance in K2SO4 and Na2SO4 Electrolytes. *Russian Journal of Electrochemistry*, *55*(9). https://doi.org/10.1134/S1023193519070115

Masukume, M., Onyango, M. S., & Maree, J. P. (2014). Sea shell derived adsorbent and its potential for treating acid mine drainage. *International Journal of Mineral Processing*, *133*, 52–59. https://doi.org/10.1016/j.minpro.2014.09.005

Mosoarca, G., Vancea, C., Popa, S., Gheju, M., & Boran, S. (2020). Syringa vulgaris leaves powder a novel low-cost adsorbent for methylene blue removal: isotherms, kinetics, thermodynamic and optimization by Taguchi method. *Scientific Reports*, *10*(1). https://doi.org/10.1038/s41598-020-74819-x

Núñez-Gómez, D., Lapolli, F. R., Nagel-Hassemer, M. E., & Lobo-Recio, M. Á. (2020). Optimization of Fe and Mn Removal from Coal Acid Mine Drainage (AMD) with Waste Biomaterials: Statistical Modeling and Kinetic Study. *Waste and Biomass Valorization*, *11*(3). https://doi.org/10.1007/s12649-018-0405-8

Panda, H., Tiadi, N., Mohanty, M., & Mohanty, C. R. (2017). Studies on adsorption behavior of an industrial waste for *removal* of chromium from aqueous solution. *South African Journal of Chemical Engineering*, *23*. https://doi.org/10.1016/j.sajce.2017.05.002

Purnamaningsih, N., Retnaningrum, E., & Wilopo, W. (2017). Pemanfaatan Konsorsium Bakteri Pereduksi Sulfat *dan* Zeolit Alam dalam Pengendapak Logam Mn. *Jurnal Penelitian Saintek*, *22*(1). https://doi.org/10.21831/jps.v22i1.15311

Rambabu, K., Banat, F., Pham, Q. M., Ho, S. H., Ren, N. Q., & Show, P. L. (2020). Biological remediation of acid mine drainage: *Review* of past trends and current outlook. *Environmental Science and Ecotechnology*, *2*, 100024. https://doi.org/10.1016/j.ese.2020.100024

Sadegh, H., & Ali, G. A. M. (2018). *Potential Applications of Nanomaterials in Wastewater Treatment*. *June*, 51–61. https://doi.org/10.4018/978-1-5225-5754-8.ch004

Suliestyah, Novi Hartamai, P., Permata Sari, I., & Alexander, E. (2021). The Fe (II) and Mn (II) adsorption in acid mine drainage using various granular sizes of activated carbon and temperatures. *IOP Conference Series: Earth and Environmental Science*, *882*(1). https://doi.org/10.1088/1755-1315/882/1/012065

Utama, S., Kristianto, H., & Andreas, A. (2016). Adsorpsi Ion Logam Kromium (Cr (Vi)) Menggunakan Karbon Aktif dari Bahan Baku Kulit Salak. *Prosiding Seminar Nasional Teknik Kimia "Kejuangan,"* 1–6.

Yan, H., Li, H., Tao, X., Li, K., Yang, H., Li, A., Xiao, S., & Cheng, R. (2014). Rapid removal and separation of iron(II) and manganese(II) from micropolluted water using magnetic graphene oxide. *ACS Applied Materials and Interfaces*, *6*(12). https://doi.org/10.1021/am502377n

Yulianis, Y., Husna, R., Zulva, N. D. I., & Mahidin, M. (2022). Adsorpsi Ion Logam Fe3+ dalam Air Asam Tambang Menggunakan Nano Zeolit Alam. *Indonesian Mining Professionals Journal*, *4*(1). https://doi.org/10.36986/impj.v4i1.51

Yushin, N., Zinicovscaia, I., Cepoi, L., Chiriac, T., & Mitina, T. (2019). Study of chemistry of CR(VI)/Cr(III) biosorption from batch solutions and electroplating industrial effluent using cyanobacteria spirulina platensis. *Revue Roumaine de Chimie*, *64*(2). https://doi.org/10.33224/rrch/2019.64.2.07

Zhan, W., Xu, C., Qian, G., Huang, G., Tang, X., & Lin, B. (2018). Adsorption of Cu(ii), Zn(ii), and Pb(ii) from aqueous single and binary metal solutions by regenerated cellulose and sodium alginate chemically modified with polyethyleneimine. *RSC Advances*, *8*(33). https://doi.org/10.1039/c8ra02055h

Zhang, Y., Zhao, J., Jiang, Z., Shan, D., & Lu, Y. (2014). Biosorption of Fe(II) and Mn(II) ions from aqueous solution by rice husk ash. *BioMed Research International*, *2014*. https://doi.org/10.1155/2014/973095